Partial Differential Equations in Applied Mathematics 11 (2024) 100792

Contents lists available at ScienceDirect

Partial Differential Equations in Applied Mathematics

journal homepage: www.elsevier.com/locate/padiff

The study of stability analysis of the Ebola virus via fractional model ☆

Renna D. Abdul-Wahhab [a], Mohannad M. Eisa [b], Sanaa L. Khalaf [a,*]

[a] Department of Mathematics, College of Science, University of Basrah, Basrah, Iraq
[b] Department of Mathematics, College of Education for Pure Science, University of Basrah, Basrah, Iraq

ARTICLE INFO

Keywords:
Ebola virus
Basic reproduction number
Disease-free equilibrium
Stability analysis
Fractional Euler method

ABSTRACT

This paper presents a fractional mathematical model for analyzing the dynamics of Ebola virus diseases. The model consists of five categories: individuals with low susceptibility to the virus $S_1(t)$, individuals with high susceptibility $S_2(t)$, infected individuals $I(t)$, exposed individuals $E(t)$, and recovered $R(t)$ individuals. In this study, we have proven the positive bounded solutions for the model under consideration. Additionally, it assesses the durability of a state without disease by utilizing the fundamental reproduction number. Moreover, an examination is conducted to assess the stability of the model. In order to validate and exemplify the research, a computational model is employed, and its results correspond with the analysis outlined in the paper.

1. Introduction

Ebola virus disease, which derives its name from the Ebola River in the Democratic Republic of the Congo, is recognized as an extremely contagious illness characterized by a high fatality rate. The virus encompasses various strains that were previously identified as Ebola hemorrhagic Fever. Some individuals infected with Ebola did not exhibit bleeding symptoms, leading to the adoption of the term Ebola virus disease.[1–9] Cases of this disease have been reported since its emergence in Zaire in 1976, with a fatality rate of approximately 79% until 2008.[10] The ongoing outbreak of Ebola virus disease is impacting countries in Central and Western Africa. The initial occurrence of the Ebola virus was recorded in 1976 in northern Zaire, which is now known as the Democratic Republic of Congo.[11–16]

The epidemic caused numerous cases, with approximately 350 individuals affected, and tragically, over two-thirds of them succumbed to the infection.[10] Unfortunately, healthcare workers who cared for the patients were eventually exposed to the virus, resulting in fatalities. Over the last four decades, Africa has experienced periodic outbreaks of the Ebola virus. Out of the 20 outbreaks, excluding the one in 2014, the highest fatality rate recorded was 66.3%, although this can vary depending on the specific outbreak.[17–20] The primary mode of transmission among humans is through direct contact with bodily fluids.[21–25] Health workers and family members of infected individuals are particularly susceptible to the infection because they often lack adequate personal protective equipment.[14,15,26–31] The customary funeral practices observed in Africa, encompassing rituals such as body cleansing, physical contact, and affectionate gestures, have played a role in exacerbating the issue. The precise origin of the virus remains uncertain; however, it is widely hypothesized that fruit bats of the Pteropodidae family serve as the primary reservoir for the Ebola virus. Furthermore, it is widely believed that transmission can occur through direct contact with primates such as monkeys, gorillas, and chimpanzees. Nevertheless, the predominant method of human-to-human transmission occurs via direct contact with the bodily fluids of an infected individual. In contrast to influenza, Ebola does not possess an airborne transmission mechanism, nor does it propagate through ingestion of contaminated food or water, as observed in other diseases like cholera, dysentery, or typhoid.

Furthermore, it is crucial to acknowledge that the transmission of the Ebola virus does not occur during the incubation period, denoting the interval between the primary infection and the manifestation of symptoms. The duration of this period for the Ebola virus typically ranges from 2 to 21 days. Therefore, in the event that an individual has been in close proximity to an Ebola patient or an individual suspected of being infected with Ebola, and subsequently experiences the onset of fever, it is imperative that immediate actions, including isolation, provision of medical treatment, and appropriate management by healthcare facilities, are undertaken in order to effectively halt the spread of the outbreak. Nevertheless, even following the individual's recuperation from the ailment, the presence of the virus in bodily fluids may persist for a prolonged duration. A study revealed the detection of the Ebola virus in the seminal fluid of a patient even after

☆ This is draft manuscript.

* Corresponding author.
E-mail addresses: rana.abdul_wahhab@uobasrah.edu.iq (R.D. Abdul-Wahhab), mohannad.eisa@uobasrah.edu.iq (M.M. Eisa), sanaasanaa1978@yahoo.com (S.L. Khalaf).

https://doi.org/10.1016/j.padiff.2024.100792
Received 20 October 2023; Received in revised form 4 June 2024; Accepted 28 June 2024
Available online 2 July 2024

a period of three months following their convalescence. Therefore, it is imperative to verify the absence of the Ebola virus prior to discharging the patient from isolation. Although there is currently a lack of widely acknowledged treatments or vaccines for Ebola, effective management of symptoms and the implementation of rigorous quarantine measures are deemed adequate in preventing the transmission of the virus.

Based on empirical investigations, the duration of the incubation period for Ebola virus disease spans a range of 2 to 21 days. During this temporal interval, the virus infiltrates cellular entities, undergoes replication, and subsequently exits the infected cells. The aforementioned procedure leads to the synthesis of EBOV glycoproteins, which subsequently bind to the endothelial lining of blood vessels, thereby increasing their permeability. Consequently, the blood vessels commence to exhibit blood leakage. Furthermore, the viral pathogen selectively infects the host's immune cells, exploiting them as a conduit for dissemination to various anatomical sites, such as the liver, kidney, and brain. The infection precipitates organ failure, ultimately culminating in the mortality of the afflicted individual.

Mathematical models have helped study infectious disease transmission dynamics like Ebola. The academic study proposes a mathematical framework to estimate the fundamental reproduction number of the Ebola virus without active control measures. The researchers also use education, contact tracing, and quarantine to improve disease containment. A mathematical model was proposed by Baize[11] to understand the Ebola virus. According to the model, the population being studied can be divided into two groups: community residents and hospital patients. The model considers key disease transmission factors. Factors affecting Ebola transmission include community-provider interactions, deceased individuals' influence, and traditional beliefs and customs.[1,32]

Fractional differential equations (FDEs) provide a precise representation of the dynamics observed in epidemiological models by incorporating factors such as population memory and learning mechanisms, which play a critical role in influencing the transmission of diseases. The locality of the integer derivative is a widely recognized characteristic, whereas the non-locality of the fractional order differential operator has been established in previous studies. This implies that the future state of the fractional order system is influenced by both its present state and all past states. The proposed approach exhibits a higher degree of realism, and the outcomes obtained from the fractional systems possess a broader scope and applicability. The inclusion of fractional derivatives within the systems introduces additional complexity, rendering analytical solutions challenging to obtain. As a result, numerical methods are employed to solve these problems. For further elaboration, please refer to the sources cited as Refs. 7, 11. On the contrary, ordinary differential equations are devoid of this capability, thus rendering them incapable of achieving this objective. Moreover, FDEs exhibit a greater extent of stability in comparison to ordinary differential equations (ODEs). In addition, it is worth noting that the fractional derivative, in contrast to the classical derivative, is characterized as a non-local operator. This implies that in the context of describing epidemic models utilizing FDEs, the incorporation of all historical and current states is considered, leading to a more accurate and inclusive depiction. Multiple definitions of fractional derivatives exist, but the Caputo derivative is commonly favored by researchers when dealing with mathematical models that incorporate FDEs. The reason behind this preference can be attributed to the inclusion of integer order derivatives in the initial conditions of FDEs with Caputo derivatives. These derivatives possess physical interpretations, such as distance, speed, and acceleration. Consequently, FDEs utilizing Caputo derivatives are extensively employed in various practical situations. The subsequent sections of the essay are organized in the following manner: Section 2 provides the definitions and properties of basic concepts related to fractional calculus. Section 3 includes the formulation of the Ebola virus fractional model. Section 4: Sensitivity Analysis In Section 5, we study Hyers–Ulam stability. Section 6 provides a numerical simulation of the Ebola virus fractional model. The last section culminates with a concise collection of concluding reflections.

2. Basic concepts

This section aims to present pertinent information regarding FDEs. It encompasses the Riemann–Liouville fractional integral, the definition of the Caputo fractional derivative, the existence and uniqueness of solutions to FDEs, and significant properties and theorems pertaining to stability analysis.

Definition 2.1 (*Ref. 33*)**.** The right and left Caputo fractional derivative, denoted by $D_{\pm}^{\alpha}$, where $m-1<\alpha<m$ and $m\in\mathbb{N}$, is defined as follows:

$$ {}_{t}^{C}D_{b}^{\alpha}x(t)=\frac{(-1)^{m}}{\Gamma(m-\alpha)}\int_{t}^{b}(\eta-t)^{m-\alpha-1}x^{(m)}(\eta)\,d\eta, \tag{2.1}$$

$$ {}_{a}^{C}D_{t}{}^{\alpha}x(t)=\frac{1}{\Gamma(m-\alpha)}\int_{a}^{t}(t-\eta)^{m-\alpha-1}x^{(m)}(\eta)\,d\eta, \tag{2.2}$$

respectively.

Lemma 2.1 (*Ref. 34*)**.** *Consider the Caputo fractional differential equation given by:*

$$\begin{cases} {}_{a}^{C}D_{t}^{\alpha}x(t)=f(t,x(t)) \\ x(t_0)=x_0 \end{cases} \tag{2.3}$$

with $0<\alpha\leq 1$. *The system* (2.3) *has equilibrium point* x^* *if* $f(t,x^*)=0$.

Theorem 2.1 (*Ref. 35*)**.** *The system denoted by Eq.* (2.3) *exhibits local asymptotic stability. If all the eigenvalues* λ *of the Jacobian matrix of Eq.* (2.3) *satisfy the following condition:*

$$|\arg(\lambda)|>\frac{\alpha\pi}{2} \tag{2.4}$$

Definition 2.2 (*Ref. 33*)**.** The Laplace transform $G(s)$ of the Caputo derivative applied to a given function $G(t)$ can be defined as follows:

$$L\{{}_{a}^{C}D_{t}^{\alpha}\,G(t),\,s\}=s^{\alpha}G(s)-\sum_{i=0}^{m-1}s^{\alpha-i-1}G^{(i)}(0)\ ,\quad \alpha\in(m-1,m),\ m\in\mathbb{N} \tag{2.5}$$

Definition 2.3 (*Ref. 33*)**.** The function $E_{r,n}(t)$ for $t\in\mathbb{R}$ is defined by

$$E_{r,n}(t)=\sum_{i=0}^{\infty}\frac{t^{i}}{\Gamma(ri+n)}\quad ,\qquad r,n>0 \tag{2.6}$$

The function $E_{r,n}(t)$ is commonly referred to as the generalized Mittag-Leffler function and it fulfills the following condition:

$$E_{r,n}(t)=\frac{1}{\Gamma(n)}+t\,E_{r,r+n}(t)\ ,\qquad n,r>0 \tag{2.7}$$

$$L\{t^{n-1}E_{r,n}(\pm\beta t^{r})\}=\frac{s^{r-n}}{s^{r}\mp\beta} \tag{2.8}$$

Where L is the Laplace transform of $E_{r,n}(t)$.

3. Formulation of the Ebola virus fractional model

The proposed fractional model for Ebola involves the partitioning of the total human population, represented as $N(t)$, into five separate compartments that are mutually exclusive. The population that is susceptible to a particular condition is divided into two subclasses: individuals with a low risk of susceptibility, represented as $S_1(t)$, and individuals with a high risk of susceptibility, represented as $S_2(t)$. In addition, the model takes into account individuals who have been exposed ($E(t)$), individuals who have been infected ($I(t)$), and individuals who have recovered ($R(t)$). In fact, the sum of these component satisfy the following equation:

$$N(t)=S_1(t)+S_2(t)+E(t)+I(t)+R(t) \tag{3.1}$$

People who have a high risk of catching the $S_2(t)$ virus from infected people make up the first susceptible population.[26,36] These categories include those involved in the burial process, healthcare workers, and infected individuals' relatives. The remaining portion of the population, $S_1(t)$, is regarded as having a minimal chance of contracting the virus. Susceptible individuals are continuously added to the population through birth and immigration at a steady rate π. It is assumed that the parameter (τ) represents the proportion of recruited individuals who are considered to be at a high risk of contracting the infection. On the other hand, the complementary fraction of individuals, represented as $(1-\tau)$, is classified as having a low likelihood of contracting the disease. The infection rate for the low-risk vulnerable population is denoted as λ, while the infection rate for the high-risk population is denoted as $\epsilon\lambda$, where ϵ represents the class modification parameter. The mortality rate μ is decreased by natural death in all five classes, with the exception of the infected class, which experiences an additional mortality rate δ attributed to infection.

The population of the group of individuals who have been exposed to the disease exhibits growth when two susceptible populations, denoted as S1 and S2, become infected as a result of interacting with individuals who are already infected. The observed increase takes place at rates denoted by ϵ and $\epsilon\lambda$, respectively. The level of exposure within a population declines as individuals begin to exhibit symptoms of the disease, with a rate denoted as ρ. The size of the infected class increases when individuals who have been exposed to the infection start showing symptoms, and this growth occurs at a rate denoted by the symbol ρ. The decline in the total population is attributed to both natural deaths, denoted by the rate μ, and deaths resulting from the disease, denoted by the rate δ. Moreover, the size of the infected population decreases due to either mortality or recovery from the infection, which happens at a rate represented by the symbol φ. The formulation of the system of fractional differential equations is derived from the assumptions given and the schematic diagram provided. The aforementioned formulation is expressed through the following equations:

$$\begin{aligned}
&{}_0^C D_t^\alpha S_1 = \pi^\alpha(1-\tau) - \lambda^\alpha S_1 I - \mu^\alpha S_1,\\
&{}_0^C D_t^\alpha S_2 = \pi^\alpha\tau - \epsilon\lambda^\alpha S_2 I - \mu^\alpha S_2,\\
&{}_0^C D_t^\alpha E = \lambda^\alpha S_1 I + \epsilon\lambda^\alpha S_2 I - \mu^\alpha E - \rho^\alpha E,\\
&{}_0^C D_t^\alpha I = \rho^\alpha E - \mu^\alpha I - \delta^\alpha I - \varphi^\alpha I,\\
&{}_0^C D_t^\alpha R = \varphi^\alpha I - \mu^\alpha R.
\end{aligned} \tag{3.2}$$

In fact, Eq. (3.2), which models human populations, must incorporate the constraint that population sizes are always non-negative. Hence, it is crucial to take into account Eq. (3.2) within a viable interval where the non-negativity characteristic is preserved. This section will examine the concept of the invariant region, which ensures that the overall population size remains greater than or equal to zero.

Theorem 3.1. *The solution set (S_1, S_2, E, I, R), where S_1, S_2, E, I, R are real numbers, is a subset of the feasible region Ψ.*

Proof. From Eq. (3.2) the total population satisfies

$${}_0^C D_t^\alpha N(t) = {}_0^C D_t^\alpha S_1 + {}_0^C D_t^\alpha S_2 + {}_0^C D_t^\alpha E + {}_0^C D_t^\alpha I + {}_0^C D_t^\alpha R \tag{3.3}$$

$$\begin{aligned}
{}_0^C D_t^\alpha N(t) &= \pi^\alpha(1-\tau) - \lambda^\alpha S_1 I - \mu^\alpha S_1 + \pi^\alpha\tau - \epsilon\lambda^\alpha S_2 I - \mu^\alpha S_2 + \lambda^\alpha S_1 I + \epsilon\lambda^\alpha S_2 I\\
&\quad - \mu^\alpha E - \rho^\alpha E + \rho^\alpha E - \mu^\alpha I - \delta^\alpha I - \varphi^\alpha I + \varphi^\alpha I - \mu^\alpha R,
\end{aligned}$$

$$\begin{aligned}
{}_0^C D_t^\alpha N(t) &= \pi^\alpha - \mu^\alpha(S_1 + S_2 + E + I + R) - \delta^\alpha I\\
&= \pi^\alpha - \mu^\alpha N(t) - \delta^\alpha I,
\end{aligned}$$

$${}_0^C D_t^\alpha\ N(t) \le \pi^\alpha - \mu^\alpha N(t). \tag{3.4}$$

The equation presented in Eq. (2.5) yields the following subsequent equation:

$$s^\alpha L\{N(t)\} - s^{\alpha-1}N(0) \le \frac{\pi^\alpha}{s} - \mu^\alpha L\{N(t)\} \tag{3.5}$$

$$(s^\alpha + \mu^\alpha)L\{N(t)\} \le \frac{\pi^\alpha}{s} + s^{\alpha-1}N(0) \tag{3.6}$$

$$L\{N(t)\} \le \frac{s^{-1}}{s^\alpha + \mu^\alpha}\pi^\alpha + \frac{s^{\alpha-1}}{s^\alpha + \mu^\alpha}N(0). \tag{3.7}$$

Then from Eqs. (2.7) and (2.8) we get

$$\begin{aligned}
N(t) &\le \pi^\alpha t^\alpha\ E_{\alpha,\alpha+1}(-\mu^\alpha t^\alpha) + E_{\alpha,1}(-\mu^\alpha t^\alpha)N(0)\\
&= \frac{\pi^\alpha}{\mu^\alpha}\left[\mu^\alpha t^\alpha\ E_{\alpha,\alpha+1}(-\mu^\alpha t^\alpha) + E_{\alpha,1}(-\mu^\alpha t^\alpha)\right]\\
&= \frac{\pi^\alpha}{\mu^\alpha}\left[\mu^\alpha t^\alpha\ E_{\alpha,\alpha+1}(-\mu^\alpha t^\alpha\ ) - \mu^\alpha t^\alpha E_{\alpha,\alpha+1}(-\mu^\alpha t^\alpha\ ) + \frac{1}{(1)}\right].\\
&= \frac{\pi^\alpha}{\mu^\alpha}.
\end{aligned} \tag{3.8}$$

Thus, the set of possible solutions for Eq. (3.2) lies within the following region:

$$\Psi = \{(S_1, S_2, E, I, R) \in R^{+5} : 0 \le N(t) \le \frac{\pi^\alpha}{\mu^\alpha}\}. \tag{3.9}$$

In this scenario, for all values of t greater than zero, if the quantity $N(t)$ is less than or equal to the ratio of π^α to μ^α, then any solution with an initial condition in the positive real numbers raised to the power of five will remain within that specific region. Consequently, it can be observed that region Ψ remains positively invariant in relation to Eq. (3.2), thereby establishing the epidemiological significance of the model within the domain Ψ. Consequently, an adequate approach involves examining the dynamics of the model in Ψ.

3.1. Disease free equilibrium point

In order to ascertain the disease-free equilibrium point of the system (3.2), it is necessary to equate the right-hand side of the system to zero. This leads to the attainment of a state of equilibrium in which the absence of disease is observed.

$$\begin{aligned}
&\pi^\alpha(1-\tau) - \lambda^\alpha S_1 I - \mu^\alpha S_1 = 0,\\
&\pi^\alpha\tau - \epsilon\lambda^\alpha S_2 I - \mu^\alpha S_2 = 0,\\
&\lambda^\alpha S_1 I + \epsilon\lambda^\alpha S_2 I - \mu^\alpha E - \rho^\alpha E = 0,\\
&\rho^\alpha E - \mu^\alpha I - \delta^\alpha I - \varphi^\alpha I = 0,\\
&\varphi^\alpha I - \mu^\alpha R = 0.
\end{aligned} \tag{3.10}$$

The point of equilibrium without disease is determined as:

$$E_0 = (\frac{\pi^\alpha(1-\tau)}{\mu^\alpha}, \frac{\pi^\alpha\tau}{\mu^\alpha}, 0, 0, 0) \tag{3.11}$$

3.2. The basic reproduction number

The basic reproduction number, commonly denoted as $\mathfrak{R}_o$, quantifies the number of new infections produced by a solitary case within a population comprising entirely of susceptible individuals.[37] According to Eq. (3.2), the compartments that are affected by the infection are

$$\begin{aligned}
&{}_0^C D_t^\alpha E = \lambda^\alpha S_1 I + \epsilon\lambda^\alpha S_2 I - \mu^\alpha E - \rho^\alpha E,\\
&{}_0^C D_t^\alpha I = \rho^\alpha E - \mu^\alpha I - \delta^\alpha I - \varphi^\alpha I.
\end{aligned}$$

Then the system above can be written as ${}_0^C D_t^\alpha x = \tilde{F}(x) - \tilde{V}(x)$.

$$\begin{bmatrix} {}_0^C D_t^\alpha E \\ {}_0^C D_t^\alpha I \end{bmatrix} = \begin{bmatrix} \lambda^\alpha S_1 I + \epsilon\lambda^\alpha S_2 I \\ 0 \end{bmatrix} - \begin{bmatrix} \mu^\alpha E + \rho^\alpha E \\ -\rho^\alpha E + \mu^\alpha I + \delta^\alpha I + \varphi^\alpha I \end{bmatrix} \tag{3.12}$$

Where $\tilde{F}(x) = \begin{bmatrix} \lambda^\alpha S_1 I + \epsilon\lambda^\alpha S_2 I \\ 0 \end{bmatrix}$ and, $\tilde{V}(x) = \begin{bmatrix} \mu^\alpha E + \rho^\alpha E \\ -\rho^\alpha E + \mu^\alpha I + \delta^\alpha I + \varphi^\alpha I \end{bmatrix}$

The Jacobian matrices of functions $\tilde{F}(x)$ and $\tilde{V}(x)$ at point E_0 are provided as follows:

$$F(x) = \begin{bmatrix} 0 & \frac{\lambda^\alpha \pi^\alpha (1-\tau)}{\mu^\alpha} + \frac{\lambda^\alpha \epsilon \pi^\alpha \tau}{\mu^\alpha} \\ 0 & 0 \end{bmatrix}$$

And

$$V = \begin{bmatrix} \mu^\alpha + \rho^\alpha & 0 \\ -\rho^\alpha & \mu^\alpha + \delta^\alpha + \varphi^\alpha \end{bmatrix}$$

The inverse of V is given by,

$$V^{-1} = \begin{bmatrix} \frac{1}{\mu^\alpha + \rho^\alpha} & 0 \\ \frac{\rho^\alpha}{(\mu^\alpha + \rho^\alpha)(\mu^\alpha + \delta^\alpha + \varphi^\alpha)} & \frac{1}{\mu^\alpha + \delta^\alpha + \varphi^\alpha} \end{bmatrix}$$

Then

$$G = FV^{-1} = \begin{bmatrix} \frac{\rho^\alpha \lambda^\alpha \pi^\alpha (1-\tau+\epsilon\tau)}{\mu^\alpha(\mu^\alpha+\rho^\alpha)(\mu^\alpha+\delta^\alpha+\varphi^\alpha)} & \frac{\lambda^\alpha \pi^\alpha (1-\tau+\epsilon\tau)}{\mu^\alpha(\mu^\alpha+\delta^\alpha+\varphi^\alpha)} \\ 0 & 0 \end{bmatrix} \tag{3.13}$$

The matrix (3.13) yields the following eigenvalues

$$\lambda = \begin{bmatrix} \frac{\rho^\alpha \lambda^\alpha \pi^\alpha (1-\tau+\epsilon\tau)}{\mu^\alpha(\mu^\alpha+\rho^\alpha)(\mu^\alpha+\delta^\alpha+\varphi^\alpha)} \\ 0 \end{bmatrix} \tag{3.14}$$

Hence, the fundamental reproductive number $\mathfrak{R}_o$ can be expressed through the following equation:

$$\mathfrak{R}_o = \frac{\rho^\alpha \lambda^\alpha \pi^\alpha (1-\tau+\epsilon\tau)}{\mu^\alpha(\mu^\alpha+\rho^\alpha)(\mu^\alpha+\delta^\alpha+\varphi^\alpha)} \tag{3.15}$$

Theorem 3.2. *If the basic reproduction number is $\mathfrak{R}_o < 1$, the disease-free equilibrium point is locally stable. However, if the basic reproduction number $\mathfrak{R}_o > 1$, the disease-free equilibrium point becomes unstable.*

Proof. The Jacobian matrix of system (3.2) at is given by

$$J = \begin{bmatrix} -\mu^\alpha & 0 & 0 & -\frac{\lambda^\alpha \pi^\alpha (1-\tau)}{\mu^\alpha} & 0 \\ 0 & -\mu^\alpha & 0 & -\frac{\lambda^\alpha \epsilon \pi^\alpha \tau}{\mu^\alpha} & 0 \\ 0 & 0 & -(\mu^\alpha + \rho^\alpha) & \frac{\lambda^\alpha \pi^\alpha (1-\tau)}{\mu^\alpha} + \frac{\lambda^\alpha \epsilon \pi^\alpha \tau}{\mu^\alpha} & 0 \\ 0 & 0 & \rho^\alpha & -(\mu^\alpha + \delta^\alpha + \varphi^\alpha) & 0 \\ 0 & 0 & 0 & 0 & -\mu^\alpha \end{bmatrix} \tag{3.16}$$

Eigenvalues of the matrix (3.16) are $\lambda_1 = -\mu^\alpha < 0$, $\lambda_2 = -\mu^\alpha < 0$, $\lambda_3 = -\mu^\alpha < 0$,

$$\lambda_4 = \frac{-\delta^\alpha \mu^\alpha - 2(\mu^\alpha)^2 - \mu^\alpha \rho^\alpha - \mu^\alpha \varphi^\alpha}{2\mu^\alpha} + \frac{\sqrt{4\lambda^\alpha \pi^\alpha \mu^\alpha \rho^\alpha (1-\tau+\epsilon\tau) + (\mu^\alpha)^2((\delta^\alpha)^2 - 2\delta^\alpha \rho^\alpha + 2\delta^\alpha \varphi^\alpha + (\rho^\alpha)^2 - 2\rho^\alpha \varphi^\alpha + (\varphi^\alpha)^2)}}{2\mu^\alpha}$$

and

$$\lambda_5 = \lambda_4 = \frac{-\delta^\alpha \mu^\alpha - 2(\mu^\alpha)^2 - \mu^\alpha \rho^\alpha - \mu^\alpha \varphi^\alpha}{2\mu^\alpha} + \frac{\sqrt{4\lambda^\alpha \pi^\alpha \mu^\alpha \rho^\alpha (1-\tau+\epsilon\tau) + (\mu^\alpha)^2((\delta^\alpha)^2 - 2\delta^\alpha \rho^\alpha + 2\delta^\alpha \varphi^\alpha + (\rho^\alpha)^2 - 2\rho^\alpha \varphi^\alpha + (\varphi^\alpha)^2)}}{2\mu^\alpha}$$

Note that λ_1, λ_2 and λ_3 have a real negative part. Now, we will proof the λ_4 and λ_5 have a real negative part.

Since$\lambda_4 = \lambda_5$, then suppose$\lambda_4 < 0$, we get

$$\frac{-\delta^\alpha \mu^\alpha - 2(\mu^\alpha)^2 - \mu^\alpha \rho^\alpha - \mu^\alpha \varphi^\alpha}{2\mu^\alpha} + \frac{\sqrt{4\lambda^\alpha \pi^\alpha \mu^\alpha \rho^\alpha (1-\tau+\epsilon\tau) + (\mu^\alpha)^2((\delta^\alpha)^2 - 2\delta^\alpha \rho^\alpha + 2\delta^\alpha \varphi^\alpha + (\rho^\alpha)^2 - 2\rho^\alpha \varphi^\alpha + (\varphi^\alpha)^2)}}{2\mu^\alpha} < 0$$

$$\sqrt{4\lambda^\alpha \pi^\alpha \mu^\alpha \rho^\alpha (1-\tau+\epsilon\tau) + (\mu^\alpha)^2((\delta^\alpha)^2 - 2\delta^\alpha \rho^\alpha + 2\delta^\alpha \varphi^\alpha + (\rho^\alpha)^2 - 2\rho^\alpha \varphi^\alpha + (\varphi^\alpha)^2)} < \delta^\alpha \mu^\alpha + 2(\mu^\alpha)^2 + \mu^\alpha \rho^\alpha + \mu^\alpha \varphi^\alpha$$

$$4\lambda^\alpha \pi^\alpha \mu^\alpha \rho^\alpha (1-\tau+\epsilon\tau) + (\mu^\alpha)^2((\delta^\alpha)^2 - 2\delta^\alpha \rho^\alpha + 2\delta^\alpha \varphi^\alpha + (\rho^\alpha)^2 - 2\rho^\alpha \varphi^\alpha + (\varphi^\alpha)^2) < (\mu^\alpha)^2(\delta^\alpha + 2\mu^\alpha + \rho^\alpha + \varphi^\alpha)^2$$

$$\frac{4\lambda^\alpha \pi^\alpha \rho^\alpha (1-\tau+\epsilon\tau)}{\mu^\alpha} + (\delta^\alpha)^2 - 2\delta^\alpha \rho^\alpha + 2\delta^\alpha \varphi^\alpha + (\rho^\alpha)^2 - 2\rho^\alpha \varphi^\alpha + (\varphi^\alpha)^2 < (\delta^\alpha)^2 + 4\delta^\alpha \mu^\alpha + 2\delta^\alpha \rho^\alpha + 2\delta^\alpha \varphi^\alpha + 4(\mu^\alpha)^2 + 4\mu^\alpha \rho^\alpha + 4\mu^\alpha \varphi^\alpha + 2\rho^\alpha \varphi^\alpha + (\rho^\alpha)^2 + (\varphi^\alpha)^2$$

$$\frac{\lambda^\alpha \pi^\alpha \rho^\alpha (1-\tau+\epsilon\tau)}{\mu^\alpha} < \delta^\alpha \mu^\alpha + \delta^\alpha \rho^\alpha + (\mu^\alpha)^2 + \mu^\alpha \rho^\alpha + \mu^\alpha \varphi^\alpha + \rho^\alpha \varphi^\alpha$$

$$\frac{\lambda^\alpha \pi^\alpha \rho^\alpha (1-\tau+\epsilon\tau)}{\mu^\alpha} < (\mu^\alpha + \rho^\alpha)(\mu^\alpha + \delta^\alpha + \varphi^\alpha)$$

$$\frac{\lambda^\alpha \pi^\alpha \rho^\alpha (1-\tau+\epsilon\tau)}{\mu^\alpha(\mu^\alpha + \rho^\alpha)(\mu^\alpha + \delta^\alpha + \varphi^\alpha)} < 1 \tag{3.17}$$

Since $\mathfrak{R}_o = \frac{\lambda^\alpha \pi^\alpha \rho^\alpha (1-\tau+\epsilon\tau)}{\mu^\alpha(\mu^\alpha+\rho^\alpha)(\mu^\alpha+\delta^\alpha+\varphi^\alpha)}$, then from (3.16) we have $\mathfrak{R}_o < 1$. Then infection-free balance, E_0, is locally asymptotically stable.

4. Sensitivity analysis

Understanding the sensitivity of $\mathfrak{R}_o$ is crucial for pandemic control. The biological measure $\mathfrak{R}_o$ is crucial for understanding the transmission dynamics of the disease. Therefore, studying the sensitivity of $\mathfrak{R}_o$ is crucial for disease elimination and control. The sensitivity of $\mathfrak{R}_o$ to changes in parameter Θ is measured by this index. To calculate changes in all parameters in the formula of $\mathfrak{R}_o$, use partial derivatives as follows:

$$\mathrm{E}_\Theta^{\mathfrak{R}_o} = \left(\frac{\partial \mathfrak{R}_o}{\partial \Theta}\right)\left(\frac{\Theta}{\mathfrak{R}_o}\right) \tag{4.1}$$

A parameter Θ describes the basic reproductive number $\mathfrak{R}_o$. According to [?], a negative (positive) index indicates that increasing Θ results in a decrease (increase) in $\mathfrak{R}_o$. Table 2 displays the sensitivity indices for parameters: ρ, λ, π, τ, ϵ, μ, δ, and φ, based on the reproductive number in Eq. (3.15) (see Table 1).

5. Hyers–Ulam stability

In order to analyze the global stability of the fractional model (3.2), we employ the Ulam–Hyers criterion. To achieve this objective, we establish the subsequent inequality:

$$\left|{}_0^C D_t^\alpha Y(t) - \mathrm{K}(t, Y(t))\right| \le \epsilon, \quad \forall t \in [0, \mathrm{T}], \tag{5.1}$$

where $\mathrm{K}(t, Y(t))$ is the right hand side of (3.2).

Now, the value of $\tilde{Y}$ belonging to the set Ψ is a solution of Eq. (3.2) if and only if there exists a value h belonging to the set Ψ such that:

i $|h(t)| \le \epsilon$.

ii

$${}_0^C D_t^\alpha \tilde{Y}(t) = \mathrm{K}(t, \tilde{Y}(t)) + h(t), \quad \forall t \in [0, \mathrm{T}]. \tag{5.2}$$

When the fractional R-LF integral is applied to both sides of Eq. (5.2), one can obtain the following:

$$\tilde{Y}(t) = \tilde{Y}(0) + \frac{1}{\Gamma(\alpha)} \int_0^t (t-\eta)^{\alpha-1} \mathrm{K}(\eta, \tilde{Y}(\eta)) d\eta + \frac{1}{\Gamma(\alpha)} \times \int_0^t (t-\eta)^{\alpha-1} h(\eta) d\eta, \forall t \in [0, \mathrm{T}].$$

As a result of taking condition (i), we obtain

$$|\tilde{Y}(t) - \tilde{Y}(0) - \frac{1}{\Gamma(\alpha)} \int_0^t (t-\eta)^{\alpha-1} \mathrm{K}(\eta, \tilde{Y}(\eta)) d\eta| \le \frac{\epsilon}{\Gamma(\alpha)} \int_0^t (t-\eta)^{\alpha-1} d\eta, \forall t \in [0, \mathrm{T}].$$

Therefore, we get

$$|\tilde{Y}(t) - \tilde{Y}(0) - \frac{1}{\Gamma(\alpha)} \int_0^t (t-\eta)^{\alpha-1} \mathrm{K}(\eta, \tilde{Y}(\eta)) d\eta| \le \frac{\epsilon \mathrm{T}^\alpha}{\Gamma(\alpha+1)}, \quad \forall t \in [0, \mathrm{T}]. \tag{5.3}$$

Table 1
Sensitivity index table.

Parameters	Determine the sensitivity index of $\mathfrak{R}_o$ to parameters	The sensitivity index
ρ	$\frac{\alpha\mu^\alpha}{\mu^\alpha+\rho^\alpha}$	+ve
λ	α	+ve
π	α	+ve
τ	$\frac{(\epsilon-1)\tau}{1+(\epsilon-1)\tau}$	−ve
ϵ	$\frac{\epsilon\,\tau}{1+(\epsilon-1)\tau}$	+ve
μ	$3\,\frac{((\mu^\alpha)^2+(2/3\,\rho^\alpha+2/3\,\delta^\alpha+2/3\,\phi^\alpha)\mu^\alpha+1/3\,\rho^\alpha(\delta^\alpha+\phi^\alpha))\alpha}{(\mu^\alpha+\rho^\alpha)(\mu^\alpha+\delta^\alpha+\phi^\alpha)}$	+ve
δ	$-\frac{\delta^\alpha\alpha}{\mu^\alpha+\delta^\alpha+\phi^\alpha}$	−ve
φ	$-\frac{\varphi^\alpha\alpha}{\mu^\alpha+\delta^\alpha+\varphi^\alpha}$	−ve

Definition 5.1. If there exists a positive constant Ξ_g such that for any $\epsilon \geq 0$, and any $\tilde{Y}(t)$ that satisfies (5.1)and the model (3.2) has a solution $Y(t)$ that satisfies

$$\left\|\tilde{Y}(t) - Y(t)\right\|_1 \leq \epsilon\Xi_g, \quad \forall t \in [0, \mathrm{T}],$$

then the model (3.2) exhibits Hyers–Ulam stability on the interval $[0, \mathrm{T}]$

Theorem 5.1. *Let the assumptions (i) and (ii) holds for the model (3.2), and if* $\Gamma(\alpha+1) > \mathrm{T}^\alpha\hbar$ *hold. Then the model (3.2) is Hyers–Ulam stability on* $[0, T]$,

Proof.

Consider $Y(t)$ be a unique solution of model (3.2), and let $\tilde{Y}(t)$ fulfill (5.1). By utilizing the fractional R-LF integral on both sides of Eq. (3.2), we obtain

$$Y(t) = Y(0) + \frac{1}{\Gamma(\alpha)}\int_0^t (t-\eta)^{\alpha-1}\mathrm{K}(\eta, Y(\eta))d\eta, \forall t \in [0, \mathrm{T}]. \tag{5.4}$$

Now, utilizing (5.3) and (5.4), we calculate $\left\|\tilde{Y}(t) - Y(t)\right\|_1$ as follows:

$$\left\|\tilde{Y}(t) - Y(t)\right\|_1 = \left\|\tilde{Y}(t) - Y(0) - \frac{1}{\Gamma(\alpha)}\int_0^t (t-\eta)^{\alpha-1}\mathrm{K}(\eta, Y(\eta))d\eta\right\|_1$$

By incorporating the term $\frac{1}{\Gamma(\alpha)}\int_0^t (t-\eta)^{\alpha-1}\mathrm{K}(\eta, \tilde{Y}(\eta))d\eta$ through addition and subtraction, and subsequently utilizing the triangle inequality, we obtain

$$\left\|\tilde{Y}(t) - Y(t)\right\|_1 \leq \left\|\tilde{Y}(t) - Y(0) - \frac{1}{\Gamma(\alpha)}\int_0^t (t-\eta)^{\alpha-1}\mathrm{K}(\eta, \tilde{Y}(\eta))d\eta\right\|_1 + \left\|\frac{1}{\Gamma(\alpha)}\int_0^t (t-\eta)^{\alpha-1}(\mathrm{K}(\eta, \tilde{Y}(\eta)) - \mathrm{K}(\eta, Y(\eta)))d\eta\right\|_1.$$

By utilizing (5.3) and the properties of the norm, it is possible to obtain

$$\left\|\tilde{Y}(t) - Y(t)\right\|_1 \leq \frac{\epsilon\mathrm{T}^\alpha}{\Gamma(\alpha+1)} + \frac{1}{\Gamma(\alpha)}\int_0^t (t-\eta)^{\alpha-1}\left\|(\mathrm{K}(\eta, \tilde{Y}(\eta)) - \mathrm{K}(\eta, Y(\eta)))\right\|_1 d\eta$$

So, we obtain

$$\left\|\tilde{Y}(t) - Y(t)\right\|_1 \leq \frac{\epsilon\mathrm{T}^\alpha}{\Gamma(\alpha+1)} + \frac{\mathrm{T}^\alpha\hbar}{\Gamma(\alpha+1)}\left\|\tilde{Y}(t) - Y(t)\right\|_1.$$

Therefore, the inequality $\left\|\tilde{Y}(t) - Y(t)\right\|_1 \leq \Xi_g\epsilon$ holds, where $\Xi_g = \frac{\mathrm{T}^\alpha}{\Gamma(\alpha+1)-\mathrm{T}^\alpha\hbar}$. By applying Definition 5.1, we can conclude that the model (3.2) exhibits Hyers–Ulam stability over the interval $[0, \mathrm{T}]$.

6. Numerical simulation of the Ebola virus fractional model

In this section of the article, our goal is to find a numerical solution for the fractional Ebola virus model. Fractional-order differential equations have attracted the attention of many scientists[8,9] due to their relevance in studying memory and hereditary aspects of various biological components. These equations are also closely connected to fractal theory. By expanding the scope of classical mathematical models to encompass fractional-order versions, researchers are able to introduce additional degrees of freedom and integrate the memory effect inherent in conventional models. The aforementioned benefits render fractional-order derivatives more closely akin to real-world phenomena in comparison to ordinary derivatives. In order to obtain a numerical solution for the model, we will employ the fractional Euler method (FEM) as described in the work by Ameen et al. (2020).[38] This methodology will yield a more comprehensive comprehension of the stability analysis elucidated in the preceding section. We will investigate the influence of varying fractional order values, specifically $\alpha = 1$, 0.9, 0.8, and 0.7, on stability characteristics. This inquiry will establish a robust groundwork for the analysis presented in this research.

Table 2
Parameter values in the fractional Ebola virus model.

Parameter	Value	Reference
π	400	[39]
τ	0.30450	[39]
μ	0.00004	[39]
λ	0.20000	Assumed
ϵ	0.21000	[40]
ρ	0.52390	[39]
δ	0.51100	[39]
φ	0.53660	[40]

In order to solve the fractional model (3.2) using the FEM, we divide the interval $[0, \mathrm{T}]$ into n subintervals $[(k-1)h, hk]$, $\forall k = 1, 2, 3, \ldots, n$ with $h = \frac{\mathrm{T}}{n}$, employing a particular methodology. Therefore, the equations that have been discretized are presented below.

$$S_1(t_k) = S_1(0) + \frac{h^\alpha}{\Gamma(\alpha+1)}\sum_{i=0}^{k}\chi_{k,i}[\pi^\alpha(1-\tau) - \lambda^\alpha S_1(t_i)I(t_i) - \mu^\alpha S_1(t_i)],$$

$$S_2(t_k) = S_2(0) + \frac{h^\alpha}{\Gamma(\alpha+1)}\sum_{i=0}^{k}\chi_{k,i}[\pi^\alpha\tau - \epsilon\lambda^\alpha S_2(t_i)I(t_i) - \mu^\alpha S_2(t_i)],$$

$$E(t_k) = E(0) + \frac{h^\alpha}{\Gamma(\alpha+1)}\sum_{i=0}^{k}\chi_{k,i}[\lambda^\alpha S_1(t_i)I(t_i) + \epsilon\lambda^\alpha S_2(t_i)I(t_i) - \mu^\alpha E(t_i) - \rho^\alpha E(t_i)],$$

$$I(t_k) = I(0) + \frac{h^\alpha}{\Gamma(\alpha+1)}\sum_{i=0}^{k}\chi_{k,i}[\rho^\alpha E(t_i) - \mu^\alpha I(t_i) - \delta^\alpha I(t_i) - \varphi^\alpha I(t_i)],$$

$$R(t_k) = R(0) + \frac{h^\alpha}{\Gamma(\alpha+1)}\sum_{i=0}^{k}\chi_{k,i}[\varphi^\alpha I(t_i) - \mu^\alpha R(t_i)].$$

where $\chi_{k,i} = (k-i)^\alpha - (k-1-i)^\alpha$, $\forall i = 0, 1, 2, \ldots, k$, and $\forall k = 1, 2, \ldots, n$.

Accurate numerical solutions can be obtained for a significant period of time through the utilization of the FEM. To initiate the analysis, we employed the initial conditions outlined in Table 3, along with the estimated values for the parameters specified in Table 2.

Figs. 1 and 2 demonstrate a decrease in the number of individuals at high risk and those low-risk susceptible over time. Likewise, Figs. 3 and 4 show a decline in the population of individuals who are exposed and infected. Additionally, Fig. 5 illustrates an increase in the number of individuals who have recovered as a result of the decreasing population of infected individuals over time.

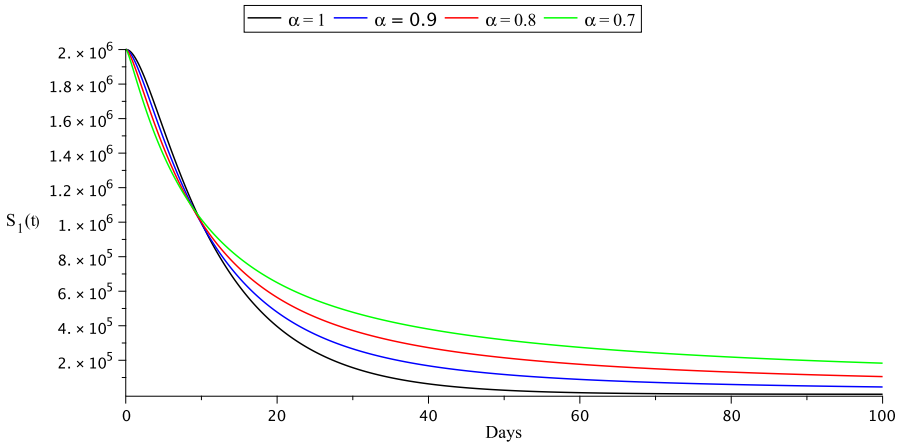

Fig. 1. The low-risk susceptible individuals $S_1(t)$.

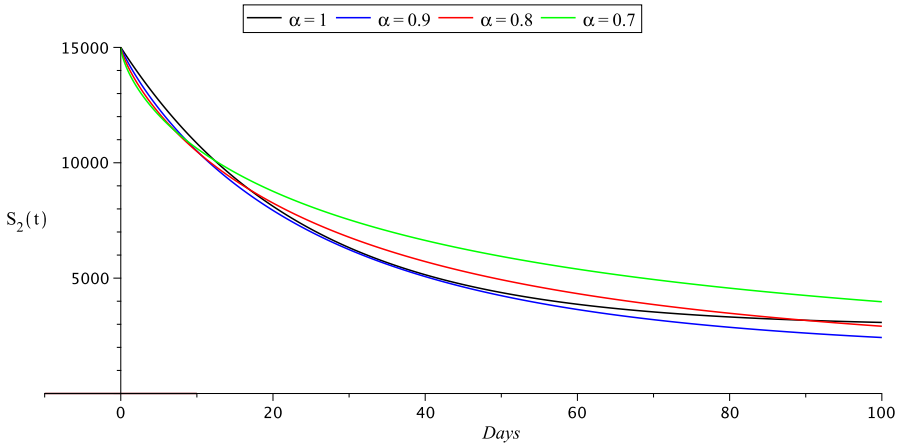

Fig. 2. The high-risk susceptible individuals $S_1(t)$.

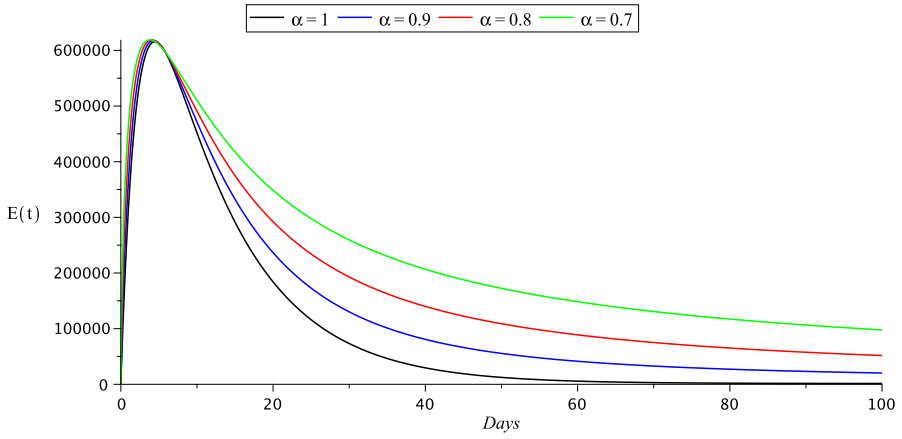

Fig. 3. The exposed individuals $E(t)$.

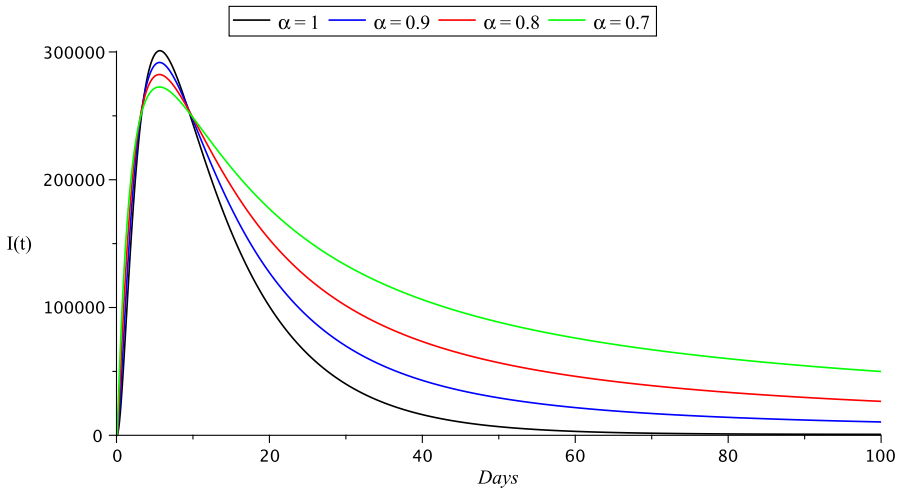

Fig. 4. The infected individuals $I(t)$.

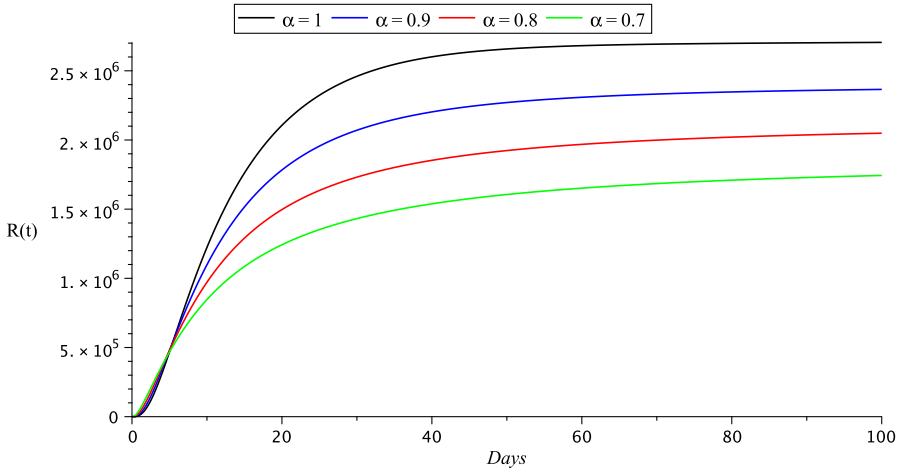

Fig. 5. The recovered individuals $R(t)$.

Table 3
The initial values in the fractional Ebola virus model.

Parameter	Value	Reference
$S_1(t)$	$S(0) = 2000000$	[41]
$S_2(t)$	$S_2(0) = 15000$	[41]
$E(t)$	$E(0) = 0$	[41]
$I(t)$	$I(0) = 0$	[41]
$R(t)$	$R(0) = 0$	[41]

7. Conclusion

This research aimed to examine the fractional model of the Ebola virus and establish several theorems concerning the existence, uniqueness, and positive stability of the solution. We extensively calculated the basic reproductive number, $\mathfrak{R}_o$, utilizing the next-generation matrix method. Additionally, we investigated the local asymptotic stability of the disease-free equilibrium. Lastly, we validated our analysis by providing a descriptive numerical simulation of the model's dynamics across different fractional order values.

Declaration of competing interest

The authors declare no financial or non-financial interests in this manuscript, including honoraria, educational grants, speakers bureaus, membership, employment, consultancies, stock ownership, or other equity interests, and expert testimony or patent-licensing arrangements.

Data availability

No data was used for the research described in the article.

References

1. Ki M. What do we really fear? the epidemiological characteristics of ebola and our preparedness. *epiH*. 2014;36:e2014014.
2. Takaidza I, Makinde OD, Okosun OK. Computational modelling and optimal control of ebola virus disease with non-linear incidence rate. *J Phys Conf Ser*. 2017;818:012003.
3. Eegunjobi AS, Makinde OD. Mathematical analysis of two strains covid-19 disease using seir model. *J Math Fundam Sci*. 2022;54(2):211–232.
4. Seidu B. Bornaa C, Makinde OD. An ebola model with hyper-susceptibility. *Chaos Solitons Fractals*. 2020;138:109938.
5. Farhood AK, Mohammed OH. Homotopy perturbation method for solving time-fractional nonlinear variable-order delay partial differential equations. *Partial Differ Equ Appl Math*. 2023;7:100513.
6. Mohammed OHFarhoodAK, Taha BA. Solving fractional time-delay diffusion equation with variable-order derivative based on shifted legendre–laguerre operational matrices. *Arab J Math*. 2023;12(3):529–539.
7. Khalaf SL, H.S. Flayyih. Analysis, predicting, and controlling the COVID-19 pandemic in Iraq through SIR model. *RICO*. 2023;10:100214.
8. Khalaf SL, Kadhim MS, Khudair AR. Studying of COVID-19 fractional model: Stability analysis. *Partial Differ Equ Appl Math*. 2023;7:100470.

9. Lazima ZA, Khalaf SL. Optimal control design of the in-vivo HIV fractional model. *Iraqi J Sci*. 2022;63(9):3877–3888.
10. Suchar VA, Aziz N, Bowe A, Burke A, Wiest MM. An exploration of the spatiotemporal and demographic patterns of ebola virus disease epidemic in West Africa using open access data sources. *Appl Geogr*. 2018;90:272–281.
11. Baize S, Pannetier D, Oestereich L, et al Emergence of zaire ebola virus disease in guinea New England. *J Med*. 2014;371(15):1418–1425.
12. Asamoah JKK, Fatmawati. A fractional mathematical model of heartwater transmission dynamics considering nymph and adult amblyomma ticks. *Chaos Solitons Fractals*. 2023;174:113905.
13. Addai E, Zhang L, Preko AK, Asamoah JKK. Fractional order epidemiological model of sars-cov-2 dynamism involving alzheimers disease. *Healthc Anal*. 2022;2:100114;
Adom-Konadu A, Bonyah E, Sackitey AL, Anokye M, Asamoah JKK. A fractional order monkeypox model with protected travelers using the fixed point theorem and newton polynomial interpolation. *Healthc Anal*. 2023;3:100191.
14. Mohammed JK, Khudair AR. Solving nonlinear stochastic differential equations via fourth-degree hat functions. *RICO*. 2023;12:100291.
15. Mohammed JK, Khudair AR. Integro-differential equations: Numerical solution by a new operational matrix based on fourth-order hat functions. *Partial Differ Equ Appl Math*. 2023;8:100529.
16. Mohammed JK, Khudair AR. Numerical solution of fractional integro-differential equations via fourth-Degree hat functions. *Iraqi J Comput Sci Math*. 2023;4(2):10–30.
17. Kerkhove MDV, Bento AI, Mills HL, Ferguson NM, Donnelly CA. A review of epidemiological parameters from ebola outbreaks to inform early public health decision-making. *Sci Data*. 2015;2(1):150019.
18. Asamoah JK, Addai E, Arthur YD, Okyere E. A fractional mathematical model for listeriosis infection using two kernels. *Decis Anal*. 2023;6:100191.
19. Jalil AFA, Khudair AR. Toward solving fractional differential equations via solving ordinary differential equations. *Comput Appl Math*. 2022;41(1):37. 12pp.
20. Khudair AR. Reliability of adomian decomposition method for high order nonlinear differential equations. *Appl Math Sci*. 2013;7:2735–2743.
21. Leroy EM, Epelboin A, Mondonge V, et al Human ebola outbreak resulting from direct exposure to fruit bats in luebo, democratic Republic of Congo, 2007. *J Vector Borne Dis*. 2009;9(6):723–728.
22. Zhang L, Addai E, Ackora-Prah J, Arthur YD, Asamoah JKK. Fractional-order ebola-malaria coinfection model with a focus on detection and treatment rate. *Comput Math Methods Med*. 2022;2022:1–19.
23. Asamoah JKK, Sun GQ. Fractional caputo and sensitivity heat map for a gonorrhea transmission model in a sex structured population. *Chaos Solitons Fractals*. 2023;175:114026.
24. Asamoah JKK, Okyere E, Yankson E, et al Non-fractional and fractional mathematical analysis and simulations for q fever. *Chaos Solitons Fractals*. 2022;156:111821.
25. Khalaf SL, Khudair AR. Particular solution of linear sequential fractional differential equation with constant coefficients by inverse fractional differential operators. *Differ Equ Dyn Syst*. 2017;25(3):373–383.
26. Neves HCC, Souza ACSe, Medeiros M, et al Safety of nursing staff and determinants of adherence to personal protective equipment. *Rev Lat-Am Enferm*. 2011;19(2):354–361.
27. MA Y, Wang Z. Bifurcation and exact solutions of space–time fractional simplified modified camassa holm equation. *Fractals*. 2023;31(07):23500858.
28. Mohammed JK, Khudair AR. A novel numerical method for solving optimal control problems using fourth-degree hat functions. *Partial Differ Equ Appl Math*. 2023;7:100507.
29. Mahdi NK, Khudair AR. Stability of nonlinear $q-$fractional dynamical systems on time scale. *Partial Differ Equ Appl Math*. 2023;7:100496.
30. Mahdi NK, Khudair AR. The delta $q-$fractional gronwall inequality on time scale. *RICO.*. 2023;12:100247.
31. Mohammed JK, Khudair AR. Solving volterra integral equations via fourth-degree hat functions. *Partial Differ Equations Appl Math*. 2023;7:100494.
32. Young TC. Comparison of two ebola hemorrhagic fever outbreaks: Uganda 2000-01 and Republic of the Congo 2001-02. *JoGH*. 2013;3(2):1–5.
33. Lin W. Global existence theory and chaos control of fractional differential equations. *J Math Anal Appl*. 2007;332(1):709–726.
34. Silva CJ, Torres DF. Stability of a fractional HIV/AIDS model. *Math Comput Simulation*. 2019;164:180–190.
35. Ahmed E, Elgazzar A. On fractional order differential equations model for nonlocal epidemics. *Physica A*. 2007;379(2):607–614.
36. Makinde O, Okosun K. Impact of chemo-therapy on optimal control of malaria disease with infected immigrants. *Biosyst*. 2011;104(1):32–41.
37. Diekmann O, Heesterbeek JAP, Roberts MG. The construction of next-generation matrices for compartmental epidemic models. *J R Soc Interface*. 2009;7(47):873–885.
38. Ameen I, Baleanu D, Ali HM. An efficient algorithm for solving the fractional optimal control of SIRV epidemic model with a combination of vaccination and treatment. *Chaos Solitons Fractals*. 2020;137:109892.
39. Agusto FB, Teboh-Ewungkem MI, Gumel AB. Mathematical assessment of the effect of traditional beliefs and customs on the transmission dynamics of the 2014 ebola outbreaks. *BMC Med.*. 2015;13(1):1–17.
40. Nuño M, Reichert TA, Chowell G, Gumel AB. Protecting residential care facilities from pandemic influenza. *Proc Natl Acad Sci*. 2008;105(30):10625–10630.
41. Sule A, Lawal J. Mathematical modeling and optimal control of ebola virus disease (EVD). *Annu Res Rev Biol*. 2018;22(2):1–11.